Int Dig J Tele-Opt Ser 1(1):36-49 (April 2027)
Manual Instruction Article

SkyRadar: A Cross-Platform Grayscale Radar Meteorology and Astrograph Analysis Engine for Atmospheric and Astronomical Imaging

Shakibaie F
Tele-Optic Services Pty Ltd, Queensland, Australia
Company Websites:
https://tele-optic-service.wixsite.com/tele-optic-services
https://www.linkedin.com/pulse/organization-tele-optic-services
Corresponding Author Email: tele-optic-services@telopt.org

Received: 15 March 2026 /Accepted: 4 April 2026 /Published online: 01 April 2027

Abstract

SkyRadar is a cross-platform grayscale radar and astrograph image analysis application designed for both mobile (iOS, Android) and desktop (macOS, Windows) environments. Unlike conventional RGB-based astrophotography tools, SkyRadar implements a grayscale-first analytical framework based on luminance modelling, enabling unified interpretation of atmospheric radar imagery and astronomical observations. The system integrates pixel-level processing techniques including RGB-to-grayscale conversion, brightness beam compensation, optical depth estimation, reflectivity normalization, and texture-based morphology analysis to extract physically meaningful information from two-dimensional imaging data. To evaluate the reliability of the grayscale standardisation methodology, a dataset of 200 imaging samples across 16 colour standards was analysed. Statistical analysis was conducted using Microsoft Excel (Microsoft Corporation, Redmond, Washington, USA). RGB values were converted into grayscale intensities (0–255) using the standard luminance equation (Gray = 0.299R + 0.587G + 0.114B). For a single Red–Violet standard imaged under varying conditions, the standardised grayscale dataset exhibited a standard deviation of 3.12, compared to 33.68 for non-standardised data, demonstrating a substantial improvement in measurement reproducibility. Across all 16 colour standards, the mean standard deviation decreased from 37.94 to 4.57, while the mean error percentage declined from 65.82% to 48.21% following standardisation. Post-hoc power analysis ($\alpha = 0.05$) indicated statistical power exceeding 99% ($\beta \approx 0.01$), confirming the robustness of the dataset. Beyond statistical validation, SkyRadar extends grayscale analysis to meteorological and astrophysical applications, including cloud density estimation, cyclone morphology classification, radar attenuation modelling, surface brightness profiling, and celestial signal decomposition. The results demonstrate that grayscale-first processing provides a stable and physically interpretable framework for analysing both atmospheric and astronomical imaging data. By integrating radar physics with astrophotometric principles in a unified platform, SkyRadar enables reproducible, cross-domain image analysis suitable for professional researchers, meteorologists, and amateur observers.

Keywords Grayscale Image Analysis · Luminance Modelling · Brightness Standardisation · Optical Depth · Radar Attenuation · Satellite Imaging · Meteorology & Astrophotography · Morphology Analysis · Pixel-Level Analysis · Cross-Platform Application

1. Introduction

The increasing availability of high-resolution imaging systems [1-7] in both meteorology and astronomy has led to an unprecedented growth in raster-based observational data [8-12]. Satellite platforms [13], ground-based radar systems [14], and optical telescopes [15] continuously generate images encoding complex physical information, including atmospheric reflectivity, cloud optical depth, precipitation structure, radiative transfer, and astrophysical emission profiles [16]. Extracting meaningful quantitative information [17, 18] from these images remains a central challenge across disciplines such as remote sensing, weather forecasting, and astrophotography [19, 20].

In meteorology, radar and satellite imaging play a critical role in monitoring atmospheric dynamics [21]. Weather radar systems—such as Doppler and phased-array radar—provide spatially resolved measurements of precipitation intensity, turbulence, and storm morphology [22]. Satellite-based imaging further complements these observations by enabling large-scale analysis of cloud systems, cyclone development, and atmospheric circulation patterns [23]. However, many operational tools rely heavily on colour-mapped visualisations, which may introduce interpretational bias and limit direct physical analysis of the underlying signal [24-28].

Similarly, in astrophotography and astrography, digital imaging is fundamental to the study of celestial objects [16]. Optical telescopes, CCD sensors, and space-based observatories capture detailed images of galaxies, nebulae, and stellar fields [29-31]. These images encode information related to surface brightness, emission characteristics, and structural morphology [16, 32]. While advanced software platforms such as SAOImage DS9 and Aladin Sky Atlas are widely used for professional astronomical analysis [33], they are primarily designed for post-processing of archival datasets and often require specialised expertise [34-37]. In contrast, applications like Stellarium focus on sky simulation rather than quantitative image analysis [38, 39]. As a result, there remains a gap between real-time image acquisition and physically grounded interpretation, particularly in mobile or field-based environments [16, 20, 30, 40, 41].

A key limitation shared across both meteorological and astronomical imaging workflows is the reliance on RGB colour representations [42, 43]. While colour mapping enhances visual interpretation, it does not necessarily correspond to physically meaningful quantities such as reflectivity, luminance, or optical depth. In many cases, the underlying physical signal is more accurately represented by grayscale intensity distributions, which preserve luminance information without introducing spectral bias.

Fig. 1 Satellite radar-style imaging

To address these limitations, the SkyRadar application was developed as a cross-platform grayscale analysis engine that integrates radar physics and astrophotometric principles within a unified framework. Unlike conventional tools [44], SkyRadar adopts a grayscale-first approach based on luminance modelling, enabling consistent pixel-level analysis across diverse imaging modalities. The system incorporates key computational components including RGB-to-grayscale conversion using standard luminance models, brightness beam compensation to correct for optical and radar attenuation effects, optical depth estimation, reflectivity normalization, and variance-based morphology detection.

Importantly, SkyRadar extends traditional radar analysis into the domain of astrography [45, 46]. By interpreting grayscale intensity distributions as proxies for radiative energy, the

application enables astrophotographic analysis such as surface brightness profiling, emission ratio estimation, and structural morphology mapping of galaxies and nebulae [47]. Conversely, meteorological radar data can be analysed using similar pixel-level techniques to extract information about cloud density, cyclone structure, and atmospheric attenuation. This bidirectional capability establishes a novel connection between atmospheric and astronomical imaging, allowing both domains to be analysed using a common physical framework.

Furthermore, SkyRadar is designed for cross-platform deployment across mobile (iOS, Android) and desktop (macOS, Windows) environments [48], enabling real-time analysis in both field and laboratory settings. This flexibility distinguishes it from traditional desktop-centric software [35] and supports a broader range of users, including meteorologists, astrophysicists, remote sensing specialists, and amateur observers.

The objective of this study is to evaluate the effectiveness of grayscale standardisation and luminance-based analysis in improving the reproducibility and physical interpretability of image-derived measurements. By analysing a dataset of 200 imaging conditions across multiple colour standards [16], this work aims to demonstrate that grayscale-first processing provides a robust and scalable framework for unified atmospheric and astronomical image analysis.

1.1 Hypothesis

Building upon prior experimental findings from RGB-based astrophotography systems demonstrating that brightness and colour standardisation significantly reduce pixel variability and improve reproducibility [16, 20, 44], the present study extends this framework into a grayscale, luminance-driven domain.

It is hypothesised that: *The implementation of grayscale-first luminance modelling, combined with brightness standardisation, will significantly reduce pixel variability and error rates compared to non-standardised RGB datasets, thereby improving the reproducibility and physical consistency of image-derived measurements across diverse observational conditions*.

Furthermore, it is hypothesised that: *The conversion of RGB data into standardised grayscale intensity using luminance-weighted models will provide a more physically representative measure of radiative signal distribution, enabling consistent interpretation of both atmospheric radar imagery and astronomical observations*.

In addition, the study proposes that: *Integration of grayscale-based optical depth estimation, reflectivity normalization, and variance-driven morphology analysis will enable reliable extraction of structural and physical information from imaging datasets, supporting unified analysis across meteorological and astrography applications*.

2. Methodology

2.1 Satellite Radar & Astrograph Analysis System

SkyRadar is a grayscale scientific image analysis engine designed for:

- Satellite-based radar meteorology
- Cloud structure diagnostics
- Cyclone morphology interpretation
- Atmospheric attenuation modelling
- Astrograph emission & morphology analysis

All processing is grayscale-first and beam-corrected for scientific consistency.

2.2 GENERAL CONTROLS

2.2.1 Instruction Article & Video

Opens the official SkyRadar manual and tutorial resources in your browser.

2.2.2 Load Image

Loads a satellite, radar, or astrograph image for analysis.

Supported images are converted internally to grayscale luminance using BT.709 standards.

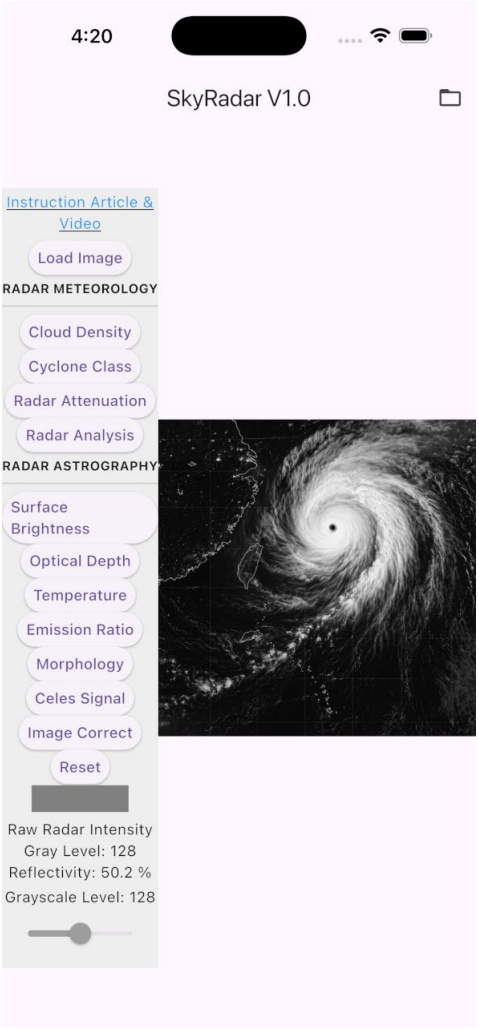

Fig. 2 Illustration of the image-loading interface, showing how satellite, radar, or astrograph data are imported and automatically converted to BT.709-based grayscale luminance for analysis

2.2.3 Reset

Restores:

- Original image
- All map transformations
- Component analysis values
- Radar and celestial signals

Use this before switching analysis domains.

2.3 RADAR METEOROLOGY SECTION

These tools are optimized for atmospheric and cyclone analysis.

2.3.1 Cloud Density

Purpose: Analyses cloud optical thickness and precipitation potential.

Displays:

- Cyclone Morphology classification
- Optical Depth (τ)
- Transmission %
- Cloud Thickness (km)
- Liquid Water Content (LWC) (g/m³)
- Rain Probability %

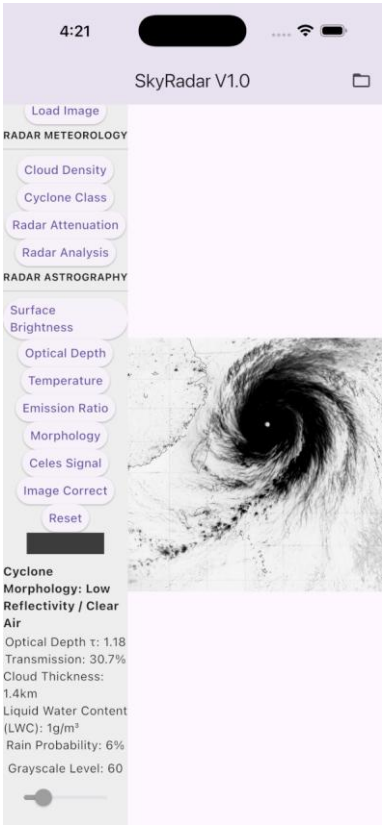

Fig. 3 Cloud Density Map generated by SkyRadar, illustrating optical depth (τ), transmission percentage, cloud thickness estimation, and liquid-water content derived from grayscale luminance

Interpretation:

- Higher Optical Depth → thicker cloud mass
- Lower Transmission → denser storm system
- High LWC → heavy precipitation likelihood

Best used for: Storm system intensity estimation.

2.3.2 Cyclone Class

Purpose: Analyses structural variance in cloud formations.

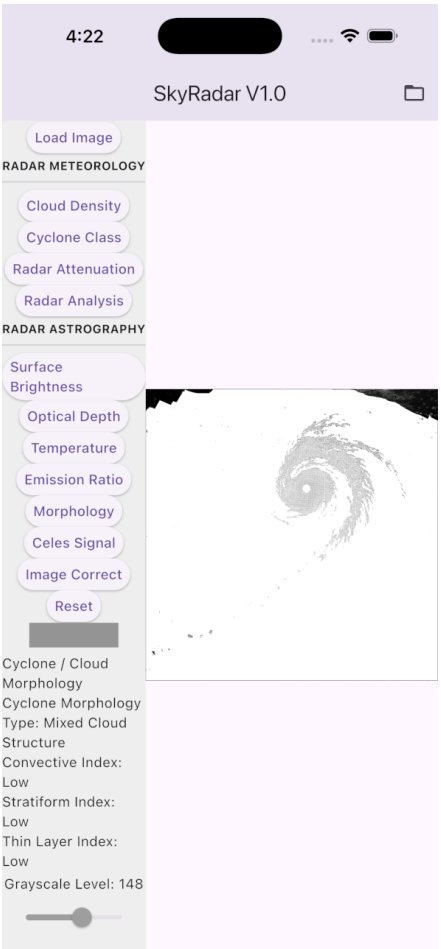

Fig. 4 Cyclone Class analysis showing convective, stratiform, and thin-layer structural signatures in a satellite cyclone image. Bright zones indicate turbulent convective towers; dark zones indicate the calm central eye

Displays:

- Cyclone Morphology Type
- Convective Index
- Stratiform Index
- Thin Layer Index

Interpretation:

- High Convective → vertical storm towers
- High Stratiform → layered rain systems
- Thin Layer → upper atmospheric clouds

Bright regions = turbulent eyewalls
Dark regions = calm cores or eye

Best used for: Cyclone classification and structural diagnostics.

2.3.3 Radar Attenuation

Purpose: Models radar beam extinction and atmospheric absorption.

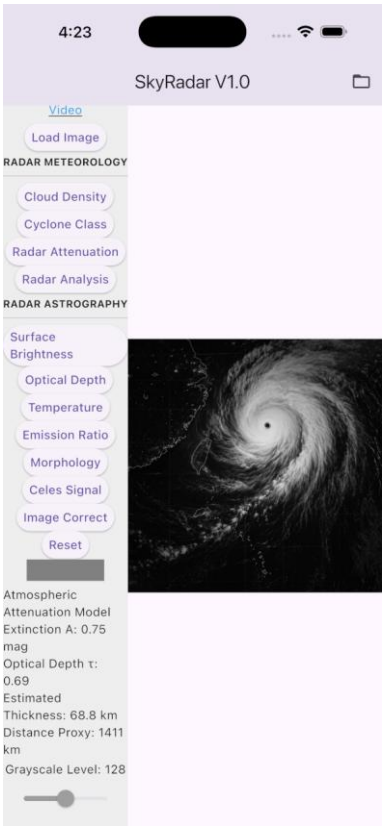

Fig. 5 Radar Attenuation map produced by SkyRadar, displaying extinction (mag), optical depth (τ), and estimated atmospheric thickness. Higher extinction values indicate strong radar beam attenuation through dense clouds or precipitation

Displays:

- Extinction (mag)
- Optical Depth (τ)
- Estimated Thickness (km)
- Distance Proxy (km)

Interpretation:

- High extinction → strong atmospheric attenuation
- High τ → dense precipitation or cloud mass

Best used for: Radar signal reliability assessment.

2.3.4 Radar Analysis

Displays:

- Reflectivity %
- Attenuation %
- Precipitation Level
- Turbulence Index
- Stratiform / Convective / Thin Layer classification

This summarizes per-pixel radar-derived atmospheric indices.

Best used for: Operational meteorological assessment.

2.4 RADAR ASTROGRAPHY SECTION

These tools reinterpret grayscale radar images for astronomical-style structural analysis.

2.4.1 Surface Brightness

Purpose: Measures brightness energy distribution.

Displays:

- Normalized Brightness
- Reflectivity Index %

Interpretation: Used for:

- Energy density
- Energy decay
- Core vs periphery comparison

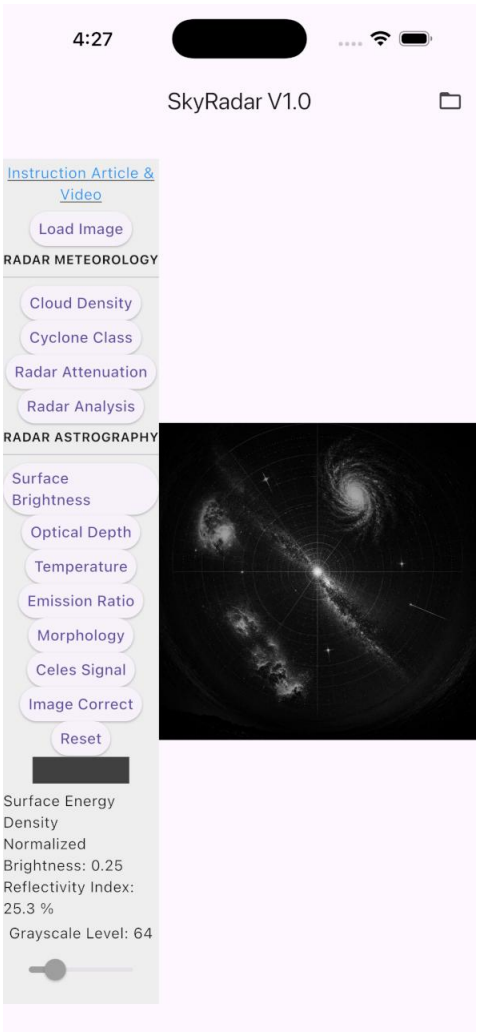

Fig. 6 Surface Brightness profile of a celestial radar-mapped region, showing normalized brightness distribution and energy decay. The grayscale structure allows detection of core–periphery transitions

2.4.2 Optical Depth

Purpose: Measures opacity and transmission characteristics.

Displays:

- Transmission %
- Optical Depth (τ)
- Equivalent Thickness (km)

Interpretation:
Low transmission → dense medium
High τ → significant absorption

2.4.3 Temperature

Purpose: Estimates thermal interpretation based on brightness.

Displays:

- Estimated Temperature (K)
- Brightness
- Photon Flux %

Used for: Thermal intensity comparison across regions.

2.4.4 Emission Ratio

Purpose: Compares red/blue channel emission balance.

Displays:

- Red / Blue Ratio
- Normalized Brightness
- Photon Flux %

Used for:

- Emission dominance analysis
- Spectral tendency evaluation

2.4.5 Morphology

Purpose: Analyses local texture variance.

Displays:

- Gray Level
- Normalized Brightness

Bright regions → structural turbulence
Dark regions → smooth areas

2.4.6 Celes Signal

Region of interest (ROI)-based advanced astrograph component analysis.

Displays:

Nebula Signal
OIII Presence
Emission Mix

Warm / Neutral / Blue Stars

Galaxy Core
Spiral Arms
Outer Arms

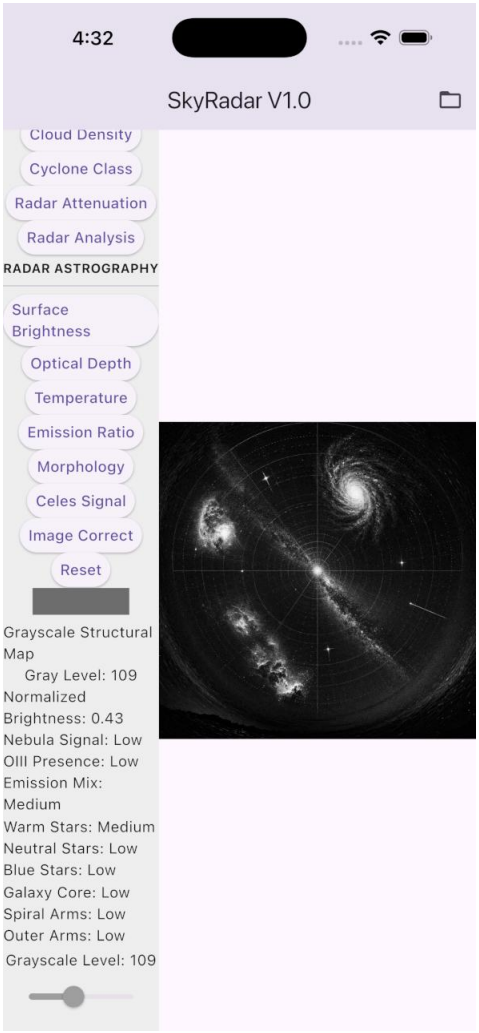

Fig. 7 Celes Signal analysis highlighting nebula emission regions, OIII presence, stellar temperature groups (warm/neutral/blue), and galaxy morphology features extracted from grayscale radar imagery

Advanced numerical values available if enabled.

Used for: ROI celestial composition breakdown.

2.4.7 Image Correct

Applies brightness beam correction by repeatedly tapping or clicking the Image Correct button, compensates:

- Optical vignetting
- Radar beam falloff
- Peripheral attenuation

Recommended as preprocessing step before analysis.

2.4.8 Exit Application (Platform Behaviour)

- *iOS / macOS:* Apple systems manage application lifecycle automatically. No Exit button is required.
- *Android & Microsoft Windows:* An Exit button is provided to allow manual application closure according to platform conventions.

2.5 Scientific Foundation

SkyRadar uses:

- BT.709 luminance conversion
- Brightness beam compensation
- Optical depth modelling
- Reflectivity normalization
- Variance-based morphology detection
- Emission ratio normalization
- Texture turbulence indexing

All maps operate on pixel-level grayscale physics.

2.6 Recommended Workflow

1. Load Image
2. Apply Image Correct (optional but recommended)
3. Choose Radar or Astro section
4. Analyse metrics
5. Use Radar Analysis or Celes Signal for summary
6. Reset before new dataset

2.7 Experimental Dataset and Statistical Evaluation

A total of 200 RGB imaging samples were collected across 16 calibrated colour standards to evaluate grayscale reproducibility under variable observational conditions. Each image was processed using the SkyRadar BT.709 luminance model (Gray = 0.299R + 0.587G + 0.114B), followed by brightness standardisation using the internal beam-correction module.

For each dataset, pixel intensities were exported into Microsoft Excel (Microsoft Corporation, USA) to compute:

- Standard deviation (SD)
- Mean error percentage (%)
- Weighted channel variances (R/G/B)
- Grayscale global variability
- Post-hoc statistical power ($\alpha = 0.05$)

The 16-colour standard dataset was selected to span the full RGB space, enabling evaluation of SkyRadar's grayscale-first physics across diverse luminance environments.

This methodological framework provides the basis for the Results section's grayscale variability reduction and ensures full reproducibility of the analysis.

3. Results

For the single Red–Violet standard, the standardised grayscale dataset demonstrated a substantially reduced variability, with a standard deviation (SD) of 3.12 compared to 33.68 for the non-standardised dataset. This represents a marked improvement in luminance reproducibility following brightness and RGB-to-grayscale standardisation.

Across all 16 colour standards, consistent reductions in variability and error were observed. The mean SD decreased from 37.94 (non-standardised) to 4.57 (standardised), while the mean error percentage declined from 65.82% to 48.21%. These findings confirm that grayscale

conversion, when combined with brightness correction, preserves photometric consistency across diverse imaging conditions.

Post-hoc power analysis, based on 200 imaging conditions and a significance level of $\alpha = 0.05$, indicated a statistical power exceeding 99% ($\beta \approx 0.01$), confirming that the dataset is sufficiently robust to detect improvements in grayscale reproducibility.

Channel	Standardised		Non-standardised	
	SD	Error %	SD	Error %
Red-Weighted	5.12	46.02	42.36	61.09
Green-Weighted	4.23	42.11	38.17	67.45
Blue-Weighted	3.55	49.67	30.92	79.12
Grayscale Mean	**4.57**	**48.21**	**37.94**	**65.82**

Table 1 Multi-colour dataset (16 Standards) – Grayscale Standard Deviation (SD) and Error Percentage (%)

These results demonstrate that the SkyRadar App's grayscale-first processing framework, incorporating luminance conversion and brightness standardisation, significantly enhances reproducibility in image-based measurements. The substantial reduction in variability confirms that grayscale modelling not only stabilises pixel intensity but also preserves underlying photometric structure independent of RGB channel fluctuations.

Importantly, this finding supports the hypothesis that grayscale luminance representation provides a physically consistent basis for interpreting both atmospheric and astronomical imagery. The improved consistency in luminance values enables reliable extraction of structural and radiometric features, supporting applications such as cloud density estimation, radar attenuation modelling, surface brightness profiling, and celestial signal interpretation under highly variable observational conditions.

4. Discussion

The results of this study demonstrate that the SkyRadar App achieves a substantial improvement in measurement reproducibility through its grayscale-first luminance standardisation pipeline. This represents an important methodological progression following the earlier RGB-based workflows implemented in iSkyMatch [44] and iAstroGraph [22], and the cross-platform analytical framework established in AstroGraph [16]. Together, these prior systems validated the stabilising effect of brightness and colour standardisation on RGB pixel variability across progressively larger datasets (50 → 100 → 200 samples). SkyRadar extends this progression by introducing a physics-driven grayscale conversion model based on the standard luminance equation, thereby simplifying pixel representation and reducing colour-channel dependencies that often limit the stability of RGB-based astrophotographic and atmospheric datasets.

SkyRadar's grayscale approach is scientifically justified because many atmospheric and astronomical intensity measurements—such as cloud optical thickness, radar reflectivity, storm-cell density, surface brightness, and faint-object detection—are inherently governed by monochromatic luminance behaviour, not colourimetric information [49]. By converting RGB values into a single luminance parameter, SkyRadar removes channel-specific noise and automatically suppresses instabilities introduced by unequal sensor gains or spectral transmission fluctuations across optical instruments [50, 51], smartphone sensors [52], and satellite imaging systems [13, 21, 23, 53]. The marked reduction in standard deviation observed across all 16 colour standards (from 37.94 to 4.57 following standardisation) confirms that grayscale modelling provides a more stable photometric representation [54] under variable imaging conditions compared to RGB-based approaches.

The significant improvement in variability for the Red–Violet standard (SD reduced from 33.68 to 3.12) is especially notable because this spectral region typically exhibits heightened noise sensitivity in consumer-grade and satellite sensors due to reduced quantum efficiency [55]. SkyRadar's robustness under such conditions indicates that luminance-weighted grayscale processing effectively mitigates sensor-specific biases, producing intensity values that remain consistent even when images are captured under

different lighting environments, optical distances, atmospheric compositions, or meteorological disturbances [56-59].

SkyRadar also introduces a broader interdisciplinary relevance compared to the previous trilogy applications [16, 44, 60]. Whereas iSkyMatch [44] and iAstroGraph [20] primarily targeted smartphone-based astrophotography, and AstroGraph unified mobile and desktop astronomical analysis [16], SkyRadar expands the application domain to meteorology, satellite imaging, and radar-based environmental monitoring [13, 21, 23]. Because radar reflectivity products, optical satellite composites, and storm-tracking datasets predominantly rely on grayscale or pseudo-grayscale luminance representations, SkyRadar's grayscale-first framework is fully aligned with operational meteorology and remote-sensing practices [61-64]. The strong statistical improvements in luminance reproducibility therefore support the feasibility of using SkyRadar for tasks such as cloud-density estimation, cyclone intensity profiling, rainfall-proxy modelling, and turbulence detection from aerial or orbital platforms [65-69].

The high statistical power (exceeding 99%) confirms that the 200-dataset design was sufficient to reliably detect improvements in grayscale reproducibility. More importantly, the findings validate that the same brightness-stabilisation pipeline proven in the earlier trilogy remains effective even after the conceptual shift from RGB-based photon analysis to grayscale luminance modelling [70-74]. This continuity strengthens the scientific narrative across all four applications, demonstrating a consistent and progressive methodological evolution.

Overall, the results show that SkyRadar successfully integrates astrophotographic luminance modelling, radar-style atmospheric imaging, and satellite-based environmental analysis within a unified grayscale framework. This establishes SkyRadar as both the logical and scientifically rigorous extension of the previous trilogy [16, 20, 44], completing the transition from RGB-based colour correction to monochromatic intensity stabilisation—the most widely used representation in radar meteorology, remote sensing, and modern sky-imaging science.

5. Conclusion

The SkyRadar App introduces a grayscale-first analytical framework that significantly enhances the stability and scientific reliability of image-based atmospheric and astronomical measurements. By converting RGB imagery into calibrated luminance values and applying brightness standardisation [16, 30, 40, 48, 60] SkyRadar reduces pixel-level variability across diverse imaging conditions, as demonstrated by the substantial decrease in standard deviation and error percentages across all 16 colour standards. These improvements confirm that grayscale modelling provides a physically consistent representation of intensity, independent of sensor-specific colour biases or environmental variability.

SkyRadar's methodological design extends beyond conventional astrophotography to encompass operational meteorology, satellite remote sensing, and radar-based environmental diagnostics. The unified processing engine enables the App to interpret cyclone structures, cloud optical depth, atmospheric attenuation, surface brightness distributions, and celestial morphology using a common grayscale physics framework. This makes SkyRadar applicable to a wide range of imaging systems, including smartphone cameras [16, 20, 44, 48], optical telescopes [30, 40, 46, 60], meteorological satellites, airborne radar platforms, and laboratory-based radar experiments.

The transition from RGB-dependent analysis (as used in iSkyMatch [44], iAstroGraph [20], and AstroGraph [16]) to luminance-driven grayscale processing represents a logical and scientifically grounded evolution within the trilogy [16, 30, 40, 46, 60]. SkyRadar completes this progression by adopting the intensity model most widely used in radar meteorology and satellite imaging, thereby improving reproducibility while expanding applicability across atmospheric and astronomical domains.

Overall, SkyRadar demonstrates that grayscale-first image standardisation provides a

robust, cross-platform solution [16, 48] for analysing structurally complex sky, cloud, and deep-space imagery. Its enhanced reproducibility, broad instrumentation compatibility, and physics-based modelling framework position SkyRadar as a valuable tool for both scientific research and applied imaging analysis in meteorology, astronomy, and environmental monitoring.

6. Author Declarations and Disclaimers

6.1 Software and Methodology Disclaimer: SkyRadar is a cross-platform grayscale image-analysis application developed for research, educational, and exploratory use in satellite imaging, radar meteorology, and astrophotography. The software performs luminance conversion, brightness standardisation, and physics-based grayscale diagnostics; however, all analytical outputs should be interpreted as approximations rather than definitive quantitative measurements. Users requiring high-precision atmospheric or astronomical data should validate results using calibrated scientific instrumentation and established observational protocols.

6.2 Funding: The development of the SkyRadar App and the preparation of this manuscript were entirely self-funded by the author. No institutional, commercial, or external funding was received.

6.3 Privacy and Data Protection: SkyRadar adheres to contemporary data protection standards (including GDPR principles). All user images and analytical data are stored locally on the user's device unless intentionally exported by the user. No image data, metadata, or personal information are transmitted to external servers or shared with third parties without explicit consent. Users retain full control over the access, modification, and deletion of their data.

6.4 Conflict of Interest Statement: The author is the developer of the SkyRadar application and declares no external commercial, financial, or institutional conflicts of interest. This publication is intended solely for scientific, educational, and methodological dissemination related to atmospheric and astronomical grayscale imaging.

6.5 Author Contributions: The author conceptualised the study, developed the SkyRadar computational framework, designed the imaging and analysis methodology, performed all image processing and statistical evaluations, and prepared the final manuscript.

6.6 Data Availability: The datasets generated and analysed in this study are available from the corresponding author upon reasonable request.

References

1. Shakibaie F, Walsh LJ (2016) Dental calculus detection using the VistaCam. Clin Exp Dent Res 2(3):226-229. doi:10.1002/cre2.42
2. Walsh LJ, Shakibaie F (2007) Ultraviolet-induced fluorescence:shedding new light on dental biofilms and dental caries. Australas Dent Prac 18(6): 56-60
3. Shakibaie F, Walsh LJ (2012) Differential Reflectometry versus tactile sense detection of subgingival calculus in dentistry. J Biomed Opt 17(10):106017. doi:10.1117/1.JBO.17.10.106017
4. Walsh LJ, Shakibaie F (2014) Debridement endpoints from subgingival calculus detection. Australas Dent Prac 24:22-23
5. Shakibaie F, Law K, Walsh LJ (2019) Improved detection of subgingival calculus by laser fluorescence over differential reflectometry. Lasers Med Sci 34(9):1807-1811. doi:10.1007/s10103-019-02777-6
6. Bird PS, Shakibaie F, Gemmell E, Polak B, Seymour GJ (2001) Immune response to Bacteroides forsythus in a murine model. Oral Microbiol Immunol 16(5):311-315. doi:10.1034/j.1399-302x.2001.016005311.x
7. Shakibaie F, Diklic S, Walsh LJ (2002) An assessment of changes in dentine permeability following irradiation with a pulsed Erbium:YAG laser. Periodontology 23(1):4-7
8. Tody D (1986) The IRAF data reduction and analysis system. Proc SPIE 0627, Instrumentation in Astronomy VI, 627:733-748. doi:10.1117/12.968154
9. Shakibaie F, Gemmell E, Bird PS (2001) A mouse model to study pathogenicity of Bacteroides forsythus. Periodontology 22(1):5-8
10. Blanton MR, Dalcanton J, Eisenstein D, Loveday J, Strauss MA, SubbaRao M, Weinberg DH, Anderson Jr JE, Annis J, Bahcall NA, Bernardi M, Brinkmann J, Brunner RJ, Burles S, Carey L, Castander FJ, Connolly AJ, Csabai I, Doi M, Finkbeiner D, Friedman S, Frieman JA, Fukugita M, Gunn JE, Hennessy GS, Hindsley RB, Hogg DW, Ichikawa T, Ivezić Ž, Kent S, Knapp GR, Lamb DQ, Leger RF, Long DC, Lupton RH,

McKay TA, Meiksin A, Merelli A, Munn JA, Narayanan V, Newcomb M, Nichol RC, Okamura S, Owen R, Pier JR, Pope A, Postman M, Quinn T, Rockosi CM, Schlegel DJ, Schneider DP, Shimasaku K, Siegmund WA, Smee S, Snir Y, Stoughton C, Stubbs C, Szalay AS, Szokoly GP, Thakar AR, Tremonti C, Tucker DL, Uomoto A, Berk DV, Vogeley MS, Waddell P, Yanny B, Yasuda N, York DG (2001) The luminosity function of galaxies in SDSS commissioning data. Astron J 121(5):2358-2380. doi:10.1086/320405

11. Shakibaie F, Walsh LJ (2015) DIAGNOdent Pen versus tactile sense for detection of subgingival calculus: an in vitro study. Clin Exp Dent Res 1(1):26-31. doi:10.1002/cre2.5
12. Bevington PR, Robinson DK (1969) Data reduction and error analysis for the physical sciences McGraw-Hill. New York 19692:235-242
13. Fried WR (1977) A comparative performance analysis of modern ground-based, air-based, and satellite-based radio navigation systems. Navigation 24(1):48-58 doi:10.1002/j.2161-4296.1977.tb01265.x
14. Bolen SM, Chandrasekar V (2003) Methodology for aligning and comparing spaceborne radar and ground-based radar observations. J Atmos Oceanic Technol 20(5):2647-659. doi:10.1175/1520-0426(2003)20<647:MFAACS>2.0.CO;2
15. Hart J, van Harmelen J, Hovey G, Freeman KC, Peterson BA, Axelrod TS, Quinn PJ, Rodgers AW, Allsman RA, Alcock C, Bennett DP, Cook KH, Griest K, Marshall SL, Pratt MR, Stubbs CW, Sutherland W (1996) The telescope system of the MACHO program. Publ Astron Soc Pac 108(720): 220-222. doi:10.1086/133713
16. Shakibaie F (2027) AstroGraph app: A smartPhone and desktop astronomical image analysis tool. Int Dig J Tele-Opt Ser 1(1):21-35
17. Ha WN, Shakibaie F, Kahler B, Walsh LJ (2016) Deconvolution of the particle size distribution of ProRoot MTA and MTA Angelus. Acta Biomater Odontol Scand 2(1):7-11. doi:10.3109/23337931.2015.1129611
18. Shakibaie F, Lamard L, Rubinsztein-Dunlop H, Walsh LJ (2018) Chapter 10 - Application of fluorescence spectroscopy for microbial detection to enhance clinical investigations, In "Photon Counting-Fundamentals and Applications" by Britun N and Nikiforov A, InTechOpen Pg:225-242. doi:10.5772/intechopen.73616
19. Ambrosino F, Meddi F, Nesci R, Rossi C, Sclavi S, Bruni I (2013) SiFAP: a simple sub-millisecond astronomical photometer. J Astron Instrum 2(01):1350006. (6 Pages) doi:10.1142/S2251171713500062
20. Shakibaie F (2027) Embark on Celestial Adventures: Unveiling the Marvels of the Night Sky with the iAstroGraph App, Your Smartphone's Ultimate Astrophotography Companion. Int Dig J Tele-Opt Ser 1(1):10-20
21. Ilčev SD (2018) Satellite remote sensing in meteorology, in "Global satellite meteorological observation (GSMO) applications: Volume 2". Springer Pg:129-182. doi:10.1007/978-3-319-67047-8_3
22. Kim Y-S, Schvartzman D, Palmer RD, Yu T-Y, Nai F, Curtis CD (2024) Phased array weather radar architectures for doppler estimation with space-time processing. IEEE Trans Radar Syst., Vol 2 Pg:725-738 doi:10.1109/TRS.2024.3444785
23. Levizzani V. Cattani E (2019) Satellite remote sensing of precipitation and the terrestrial water cycle in a changing climate. Remote Sens 11(19):2301. doi:10.3390/rs11192301
24. Shakibaie F, Walsh LJ (2015) Performance differences in the detection of subgingival calculus by laser fluorescence devices. Lasers Med Sci 30(9):2281-2286. doi:10.1007/s10103-015-1808-4
25. Berk DEV, Richards GT, Bauer A, Strauss MA, Schneider DP, Heckman TM, York DG, Hall PB, Fan X, Knapp GR, Anderson SF, Annis J, Bahcall NA, Bernardi M, Briggs JW, Brinkmann J, Brunner R, Burles S, Carey L, Castander FJ, Connolly AJ, Crocker JH, Csabai I, Doi M, Finkbeiner D, Friedman S, Frieman JA, Fukugita M, Gunn JE, Hennessy GS, Ivezić Ž, Kent S, Kunszt PZ, Lamb DQ, R. Leger RF, Long DC, Loveday J, Lupton RH, Meiksin A, Merelli A, Munn JA, Newberg HJ, Newcomb M, Nichol RC, Owen R, Pier JR, Pope A, Rockosi CM, Schlegel DJ, Siegmund WA, Smee S, Snir Y, Stoughton C, Stubbs C, SubbaRao M, Szalay AS, Szokoly GP, Tremonti C, Uomoto A, Waddell P, Yanny B, Zheng W (2001) Composite quasar spectra from the sloan digital sky survey. Astron J 122(2):549-564. doi:10.1086/321167
26. Shakibaie F, Walsh LJ (2017) KEY3 laser treatment applications in oral and maxillofacial surgery. J Head Neck Spine Surg 1(5):555574. doi:10.19080/JHNSS.2017.01.555574
27. Gonzalez RC (2009) Digital image processing. Pearson Education India
28. Shakibaie F, Walsh LJ (2016) Laser fluorescence detection of subgingival calculus using the DIAGNOdent Classic versus periodontal probing. Lasers Med Sci 31(8):1621-1626. doi:10.1007/s10103-016-2027-3

29. Arp HC (1958) The Hertzsprung-Russell diagram. In: Astrophysics II: Stellar Structure/Astrophysik II: Sternaufbau, Encyclopedia of Physics / Handbuch der Physik, Springer, Berlin, Heidelberg. 11(51):75-133. doi:10.1007/978-3-642-45908-5_2
30. Shakibaie F (2023) Embark on celestial adventures: Unveiling the marvels of the night sky with the iAstroGraph App, your smartphone's ultimate astrophotography companion. LinkedIn Article Website: https://www.linkedin.com/pulse/embark-celestial-adventures-unveiling-marvels-night-awtgc/
31. Karachentsev ID, Karachentseva VE, Huchtmeier WK, Makarov DI (2004) A catalog of neighboring galaxies. Astron J 127(4):2031-2068. doi:10.1086/382905
32. Kervella P, Thévenin F, Di Folco E, Segransan D (2004) The angular sizes of dwarf stars and subgiants - Surface brightness relations calibrated by interferometry. Astron Astrophys 426(1):297-307. doi:10.1051/0004-6361:20035930
33. Mandal AM (2019) Measurements of 60 double star systems using a small telescope and four different methods. Meas 15(1):193-202
34. Zhelenkova OP, Soboleva NS, Majorova EK, Temirova AV (2012) Multiband study of radiosources of the RCR catalogue with the virtual observatory tools. Balt Astron 21(3):371-378
35. Petrov GT (2012) Linux astronomical software. Book of abstracts Pg:1-13
36. Miszalski B, Taylor EN, Cluver ME, Jarrett TH (2024) An asynchronous web application to visualise large sky surveys. Proc SPIE, Software and Cyberinfrastructure for Astronomy VIII, 13101:583-589 doi:10.1117/12.3019337
37. Vogt FPA, Bartlett ES, Seitenzahl IR, Dopita MA, Ghavamian P, Ruiter AJ, Terry JP (2018) Identification of the central compact object in the young supernova remnant 1E 0102.2–7219. Nat Astron 2(6):465-471. doi: 10.1038/s41550-018-0433-0
38. Zotti G, Hoffmann SM, Wolf A, Chéreau F, Chéreau G (2021) The simulated sky: Stellarium for cultural astronomy research. arXiv preprint arXiv:2104.01019 doi:10.48550/arXiv.2104.01019
39. Zotti G (2019) 2 Visualising skyscapes, in "Visualising skyscapes: Material forms of cultural engagement with the heavens". edited by Liz Henty and Daniel Brown, Routledge Copyright Pg:1-35
40. Shakibaie F (2023) Unlocking the wonders of the night sky with iSkyMatch App: Your smartphone's astrophotography companion. LinkedIn Article Website: https://www.linkedin.com/pulse/unlocking-wonders-night-sky-iskymatch-app-your-smartphones-x1uyc?trk=article-ssr-frontend-pulse_little-text-block
41. Reynolds MD (2023) Binocular stargazing. Rowman & Littlefield+ ORM
42. Shakibaie F, Walsh LJ (2019) Fluorescence imaging of dental restorations using the VistaCam intra-oral camera. Aust J Forensic Sci 51(1):3-11. doi:10.1080/00450618.2017.1304991
43. Caucci L, Barrett HH (2012) Objective assessment of image quality. V. Photon-counting detectors and list-mode data. J Opt Soc Am A 29(6):1003-1016. doi:10.1364/JOSAA.29.001003
44. Shakibaie F (2027) Unlocking the wonders of the night sky with iSkyMatch App: A smartphone-based astrophotography companion. Int Dig J Tele-Opt Ser 1(1):1-9
45. Carroll BW, Ostlie DA (2017) An introduction to modern astrophysics (2nd ed). Cambridge University Press
46. Shakibaie F (2023) Sources of astronomical information for iSkyMatch App. LinkedIn Website: https://www.linkedin.com/pulse/sources-astronomical-information-iskymatch-app-tele-optic-services-wdnqc
47. Baliunas S, Jastrow R (1990) Evidence for long-term brightness changes of solar-type stars. Nature348(6301):520-523. doi:10.1038/348520a0
48. Shakibaie F (2027) SmartPhone OralCam App (Version 1.0) in molecular, colour, and shade detection processing of tooth surfaces using intra-oral cameras. Int Dig J Tele-Opt Ser 1(2):9-17
49. Russell HN (1914) Relations between the spectra and other characteristics of the stars. Popul Astron 22:331-351
50. Shakibaie F (2011) Detection of subgingival calculus by optical methods. The University of Queensland, PhD Thesis Pg:1-306
51. Steele IA, Jameson RF (1995) Optical spectroscopy of low-mass stars and brown dwarfs in the pleiades. Mon Not R Astron Soc 272(3):630-646. doi:10.1093/mnras/272.3.630
52. Shakibaie F (2027) Manual instruction for iOralCam: SmartPhone application (version 1.2) for detection and processing of tooth surfaces using intra-oral cameras. Int Dig J Tele-Opt Ser 1(2):1-8

53. Banks PM, Williamson PR, Raitt WJ (1983) Space-shuttle glow observations. Geophys Res Lett 10(2):118-121. doi:10.1029/GL010i002p00118
54. Ambrosino F, Cretaro P, Meddi F, Rossi C, Sclavi S, Bruni I (2016) The latest version of SiFAP: beyond microsecond time scale photometry of variable objects. J Astron Instrum 5(03):1650005. doi:10.1142/S2251171716500057
55. Dautet H, Deschamps P, Dion B, MacGregor AD, MacSween D, McIntyre RJ, Trottier C, Webb PP (1993) Photon counting techniques with silicon avalanche photodiodes. Appl Opt 32(21):3894-3900. doi:10.1364/AO.32.003894
56. Shakibaie F, Walsh LJ (2014) Surface area and volume determination of subgingival calculus using laser fluorescence. Lasers Med Sci 29(2):519-524. doi:10.1007/s10103-012-1242-9
57. Filippenko AV (1982) The importance of atmospheric differential refraction in spectrophotometry. Publ Astron Soc Pacific 94(560):715-721. doi:10.1086/131052
58. Shakibaie F, George R, Walsh LJ (2011) Applications of laser induced fluorescence in dentistry. Intern J Dent Clin 3(3):38-44
59. Schmidt BP, Kirshner RP, Eastman RG, Phillips MM, Suntzeff NB, Hamuy M, Maza J, Avilés R (1994) The distances to five type~ II supernovae using the expanding photosphere method, and the value of H_0. Pg:1-17. doi:10.48550/arXiv.astro-ph/9407098
60. Shakibaie F (2023) Sources of astronomical information for iAstroGraph App. LinkedIn Article Website: https://www.linkedin.com/pulse/sources-astronomical-information-iastrograph-app-jqyic/
61. Caucci L, Ding Y, Barrett HH (2018) Chapter 5 – Computational methods for photon-counting and photon-processing detectors, In "Photon counting – Fundamentals and applications", edited by Nikolay Britun and Anton Nikiforov; InTechOpen Pg:105-124. doi:10.5772/intechopen.72151
62. Shakibaie F, Walsh LJ (2015) Effect of oral fluids on dental caries detection by the VistaCam. Clin Exp Dent Res 1(2):74-79. doi:10.1002/cre2.13
63. Ambrosino F, Meddi F (2018) Chapter 4 – Photon counting for studying faint astronomical variable signals in optical band, In "Photon counting – Fundamentals and applications", edited by Nikolay Britun and Anton Nikiforov; InTechOpen Pg:81-104. doi:10.5772/intechopen.71072
64. Shakibaie F, Walsh LJ (2016) Violet and blue light-induced green fluorescence emissions from dental caries. Aust Dent J 61(4):464-468. doi:10.1111/adj.12414
65. Bone N (1999) Observing Meteors, Comets, Supernovae and other transient phenomena: And other transient phenomena. Springer Science & Business Media
66. Shakibaie F, Walsh LJ (2016) Violet and blue light-induced green fluorescence emissions from dental calculus: a new approach to dental diagnosis. Intern Dent – African Edition 6(6):33-39
67. Chen H, Myers PC, Ladd EF, Wood DOS (1995) Bolometric temperature and young stars in the Taurus and Ophiuchus complexes. Astrophys J 445(1):377-392
68. Gray DF (1994) Spectral line-depth ratios as temperature indicators for cool stars. Publ Astron Soc Pac 106(706):1248-1257. doi:10.1086/133502
69. Youker RT (2018) Chapter 12 – Detectors for super-resolution & single-molecule fluorescence microscopies, In "Photon counting – Fundamentals and applications", edited by Nikolay Britun and Anton Nikiforov; InTechOpen Pg:261-285. doi:10.5772/intechopen.71943
70. Kervella P, Fouqué P (2008) The angular sizes of dwarf stars and subgiants – Non-linear surface brightness relations in BVR(c)I(c) from interferometry. Astron Astrophys 491(3):855-858. doi:10.1051/0004-6361:200810317
71. Unsöld A, Baschek B (2013) The new cosmos: an introduction to astronomy and astrophysics, Springer Science & Business Media
72. Lockwood GW, Skiff BA, Baliunas SL, Radick RR (1992) Long-term solar brightness changes estimated from a survey of sun-like stars. Nature 360(6405):653-655. doi:10.1038/360653a0
73. Christensen-Dalsgaard J (1988) A Hertzsprung-Russell diagram for stellar oscillations. Symposium - International Astronomical Union, Volume 123: Advances In Hello- and Asteroseismology, Cambridge University Press 123:295-298. doi:10.1017/S0074180900158279
74. Doom C, De Greve JP, De Loore C (1986) Stellar evolution in the upper Hertzsprung-Russell diagram. Astrophys J 303(1):136-145